Investigation of Ultrasonic Guided Waves Interacting With Piezoelectric Transducers

Sina Fateri, *Student Member, IEEE*, Premesh Shehan Lowe, *Student Member, IEEE*,
Bhavin Engineer, and Nikolaos V. Boulgouris, *Senior Member, IEEE*

Abstract—**Ultrasonic guided waves (UGW) can be used to inspect and monitor a structure from a single test location. Piezoelectric transducers are commonly dry-coupled with force to the surface of the waveguide in order to excite UGWs. These UGWs propagating within the waveguide will interact and reflect from known features, thus possible damage could be detected. In this paper, the interaction of UGWs with piezoelectric transducers is reported and investigated. A Finite Element Analysis (FEA) approach has been used to conduct a parametric study in order to quantify the effect of the waveguide diameter on the guided wave response. Laboratory experiments are carried out to measure the effect of the force on the dry-coupled piezoelectric transducers and the corresponding guided wave response, including reflections and mode conversions. A test rig is used to apply and measure the force on the piezoelectric transducers. For verification, a 3D Laser Doppler Vibrometry (3D-LDV) scan is performed on the waveguide in order to quantitatively identify the modes of interest. The conclusions reached this paper, particularly with respect to the quantification of the wave mode properties, lead to useful recommendations which may contribute to field inspection scenarios.**

Index Terms—**Piezoelectric transducers, ultrasonic guided wave (UGW), mode conversion, transducer coupling, force.**

I. Introduction

ULTRASONIC Guided Waves (UGWs) have been used for over 20 years to inspect the health of structural components of varied geometries; principally for detection of flaws, corrosion and metal loss damage [1]. The technology is a commercially valid and rapid way of assessing large volumes of metal structures like pipes, rods, bars, rails*, etc.* from a single test location. For field inspections, UGW frequencies commonly operate at the kHz range which exhibit minimal attenuation over long distances. The reflected UGWs are measured and interpreted into defect categorization, giving parameters including total cross sectional area and through wall depth of the defect [2], [3].

Although many recent techniques are evolving into promising inspection tools, several challenges yet exist. UGW gives rise to multiple wave modes within a frequency region which can be dispersive as their velocity is frequency dependent. Therefore, signal interpretations are often difficult due to multimode propagation [4], [5]. Apart from the fundamental existing guided wave modes in a structure, the presence of higher order modes makes a further challenging scenario in inspections. The presence of the higher order flexural/longitudinal modes was known from the work of Devault and Curtis [6] and it has been further defined on different wave modes by Meitzler [7]. The curves for the higher longitudinal and flexural modes intersect the frequency axis at non zero values of frequency which are referred as the cut-off frequency [7].

Mode conversion along with waveguide geometric features can also cause a further challenge for signal interpretation. Mode conversion often occurs when UGW signal encounters a discontinuity and converts into a wave mode with different velocity and displacement characteristic. The main focus of the recent research on mode conversion phenomena has been on part circumferential notches, adhesively bonded lap joints and cracks by Alleyne *et al.* [8], Lowe *et al.* [9], Demma *et al.* [10] plates with thickness variations by Cho [11], reflections from free-edge of a structural element by Cho and Rose [12], Morvan *et al.* [13] and Jiangong *et al.* [14]. These studies are mainly focused on the mode conversion of longitudinal and/or torsional wave modes from defects, joints, thickness variations, *etc.* and no attention has been given to the possible reflections and mode conversions from the source of excitation which is the coupled transducer.

Therefore, the reflections and mode conversions of UGWs from transducers were investigated and studied via Finite Element Analysis (FEA), experimentation and 3D-LDV scans. In this study it is shown that significant reflection and mode conversion can occur due to the presence of the coupled transducers which potentially become a disruptive matter in field inspections and contribute to the coherent noise. According to the literature, these reflections and mode conversions from the transducers have not been studied and/or reported in the field.

Recently, Lowe *et al.* [15] presented a Finite Element Analysis (FEA) to investigate the UGW interaction with the source of excitation. They observed reflections and mode conversions arising from a coupled transducer and validate the FEA results empirically. They reached a closer agreement
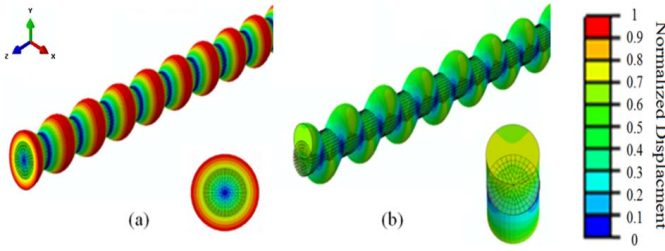
Fig. 1. Displacement characteristics of (a) L(0,1) (b) F(1,1) in isometric and cross-sectional view at 80 kHz.

between theoretical predictions and experimental results using the FEA procedure. However, in their study the main attention was given to the FEA modelling technique and little attention was given to the experimental investigation considering the effect of essential parameters such as force (on transducers) and waveguide diameter. Therefore, this paper studies the effect of the force on the piezoelectric transducers and the corresponding guided wave response considering the same waveguide, FEA layout and experimental setup as used in Lowe *et al.* [15]. The amplitude of the mode converted signal is empirically quantified. The FEA parametric study is also presented to study the effect of change in waveguide diameter on the corresponding guided wave response. Furthermore, a 3D-LDV is also used to effectively identify the propagating wave modes of interest.

The paper is organized as follows. In Section II the theoretical background is presented, Section III describes the FEA procedure for the studied problem. Laboratory experiments are detailed in Section IV and finally, conclusions are drawn in Section V.

II. THEORETICAL BACKGROUND

In this Section, we present the theoretical background upon which we will base our subsequent study of UGW modes and transducer coupling.

A. Behaviour of UGW Modes

1) L(0,1) Wave Mode: L(0,1) is an axisymmetric wave mode that has higher phase velocity compared to its accompanied non-axisymmetric mode. This wave mode is commonly termed as an attenuative and dispersive wave mode in pipe applications [16], [17]. However, in this paper according to the dispersion curves (*i.e.*, Figure 3) of the waveguide under investigation (*i.e.*, 2.15m long, *8mm diameter aluminium rod*) for the operating frequency range of interest (*i.e.*, 20 to 100kHz); the group velocity is approximately in the range of [5000:5100 *m/s*]. Therefore, throughout the paper it is nominally assumed to be non-dispersive as it experiences very low dispersion. Figure 1, illustrates a short section of each fundamental wave mode in the rod under investigation. These are standing waves calculated using a FEA procedure for dispersion curve calculation developed by Sanderson and Smith [18]. Figure 1-(a) illustrates the displacement magnitude of L(0,1) wave mode at 80 kHz which mainly exhibits axial

displacement. It is meshed using structured 8-node linear brick elements with reduced integration.

2) F(1,1) Wave Mode: First order flexural wave mode, F(1,1) is a non-axisymmetric wave mode with relatively lower phase velocity compared to its accompanied longitudinal wave mode in the frequency region of interest (*i.e.*, 20 to 100kHz). Figure 1-(b) illustrates the displacement characteristics of F(1,1) which mainly exhibits radial displacement characteristics. It is also shown in [19] and [20] that the dispersion properties of first order flexural F(1,1) wave mode can differ from other wave modes. Cui *et al.* [20] highlighted the occurrence of F(1,1) with anomalous dispersion in cylindrical systems and considered possible methods that fall into three categories as experimental, numerical and theoretical methods. They also suggested using Laser Doppler Vibrometer (LDV) to identify the modes of interest and measure their dispersion.

B. Transducer Coupling

Transducer coupling plays an important role in UGW inspections. Conventional ultrasonic liquid couplant is not used when operating transducers, as shear wave modes are not supported in Newtonian fluids. Thus dry coupling with a sufficient amount of force enables the transfer of the UGWs into the inspected substrate. The transducer needs to be bound to the surface for good coupling [21]. This can be achieved *e.g.* in pipes by wrapping an inflatable collar around the transducer rings. In commercial UGW systems, the inflatable collars are typically pressurized from 138 kPa up to 414 kPa in order to exert sufficient pressure on the transducers for them to generate the shear motion in the surface of the waveguide [22]. If the transducers are not sufficiently coupled to the surface, this will induce ringing of the transducers. Due to the lack of damping, the transducer will listen to itself resonating rather than transmitting sound into the component under inspection. This will degrade the resolution of any UGW response and make the signal interpretation challenging.

C. The Effect of Force on Transducers

Alleyne and Cawley [23] demonstrated the receiving characteristics of a dry coupled transducer. Sixteen circumferentially bonded transducer elements were used to excite UGWs at a single frequency, 70 kHz within a pipe. A clamped transducer receiver listened to the excitation from the bonded element. The peak to peak amplitude of a pulse possessing the velocity of L(0, 2) wave mode in the pipe was measured. It was shown that the magnitude of a received pulse would non-linearly increase with an increase in clamping force. This behaviour can be prescribed from various macroscopic elastic contact theories such as the *JKR model* [24] and the Greenwood and Williamson model [25] which are fundamentally based upon the *Hertzian theory of elastic contact*. It is said that the contact area between two elastic bodies is proportionally equivalent to the normal force applied to it by a power of a 1/3. In this paper we consider the force dependent coupling of transducers on an 8mm diameter aluminium rod. Therefore, the effect

TABLE I
ASSUMED MATERIAL PROPERTIES

Properties	Aluminium Rod	Transducer Element	Backing Block
Density	2700kg/m^3	7600kg/m^3	7830kg/m^3
Young's Modulus	70GPa	76GPa	207GPa
Poisson's Ratio	0.33	0.31	0.3

of force on the reflections and mode conversions from the transducers are further investigated in Section IV-B.

III. FINITE ELEMENT ANALYSIS

Lowe *et al.* [15] presented a Finite Element Analysis (FEA) to investigate the UGW interaction with the source of excitation. The same FEA technique has been used in this study to investigate the reflection and mode conversion arising once UGW interact with the transducers with an aid of a parametric study. The geometry used is an aluminium rod (8mm diameter, 2.15m long) and FEA is performed using the commercially available FE software, ABAQUS *version 6.12*. The model is a three-dimensional (3D) simulation of UGWs propagating within a solid body using linear brick elements. The excitation frequency in all models is chosen to be 80 kHz since according to the dispersion curve given in Figure 3 the individual wave modes are expected to arrive at separate Time of Arrivals (ToAs) therefore, they could be directly identified. The dispersion curves for the rod are calculated using Disperse [26]. At the excitation frequency used, there are only three possible modes, L(0,1), T(0,1) and F(1,1). The excitation direction is along the axis of the rod (the alignment of the piezoelectric is longitudinal). This would preferentially excite L(0,1) and F(1,1). Therefore the presence of T(0,1) could be neglected due to the alignment of the piezoelectric element. Material properties assumed in the FE models are illustrated in Table 1. A parametric study is undertaken through FE model in order to observe the behaviour of UGWs interacting with the transducers on different diameters aluminium rods. Therefore the ratio between the reflected and mode converted signal in relation to the waveguide diameter could be measured. The layout of the FE model is presented in Figure 2. The dispersion curve of the rod with different diameter is illustrated in Figure 3. It is notable that the velocity of L(0,1) is inversely proportional to the change in the diameter. However; as the diameter of the rod expands, the velocity of F(1,1) increases.

Figure 4 represents the UGW responses with varying diameter rods. The response for the 8 mm diameter is chosen as the baseline [15]. The dashed blue and red lines respectively represent the expected and unexpected wave modes appearing at the baseline. The dashed blue and red lines assist the reader in observing the movements of the wave modes of interest in time as the diameter of the rod increases.

According to Figure 4, after the first F(1,1) echo and second L(0,1) echo, there is an unexpected wave-packet
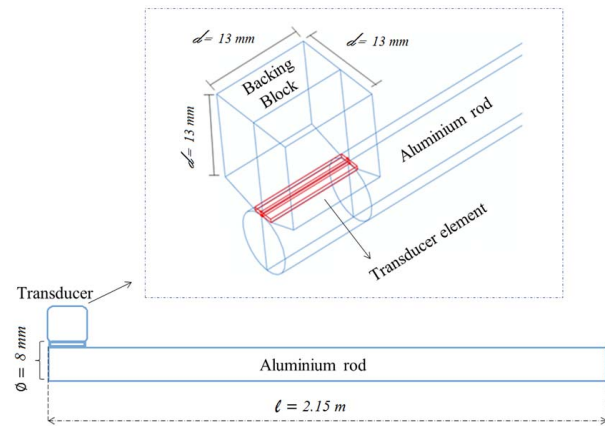

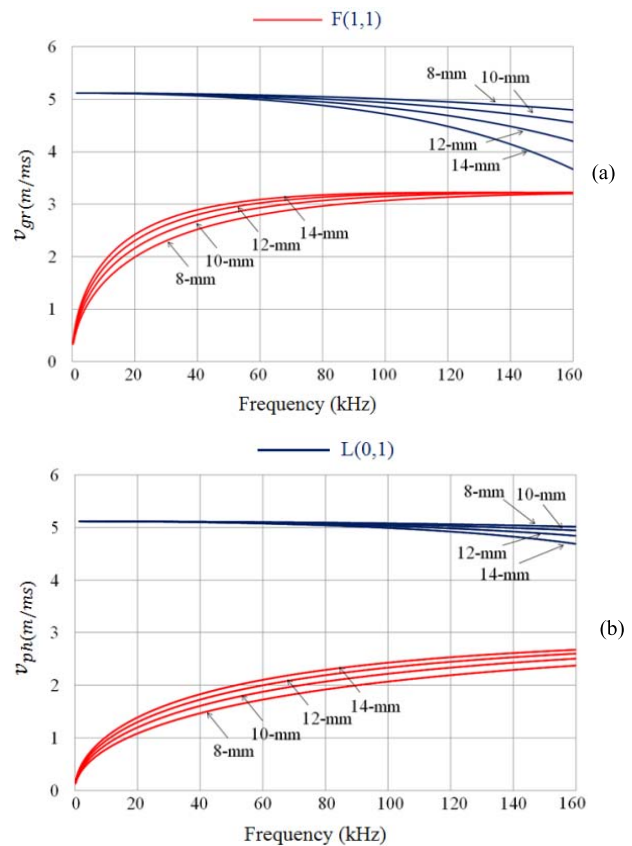Fig. 2.   Layout of the FE model and zoomed view at the excitation point.

Fig. 3.   Dispersion curve. (a) Group velocity. (b) Phase velocity for different diameter aluminium rods.

present in the UGW response for every rod diameter (from 8 mm to 14 mm). ToA of these wave-packets are consistent with mode conversions from F(1,1) to L(0,1) and/or L(0,1) to F(1,1) occuring at the transducer location [27].

Furthermore, mode conversion phenomenon is evident in all the responses where the diameter of the rod varies from 8 mm to 14 mm. It is also evident that the wave modes arrive at different ToAs due to the change in their velocity after the corresponding changes in the diameter. This causes the L(0,1) and F(1,1) wave modes to be superposed at some echoes as shown in Figure 4 (c) and (d).
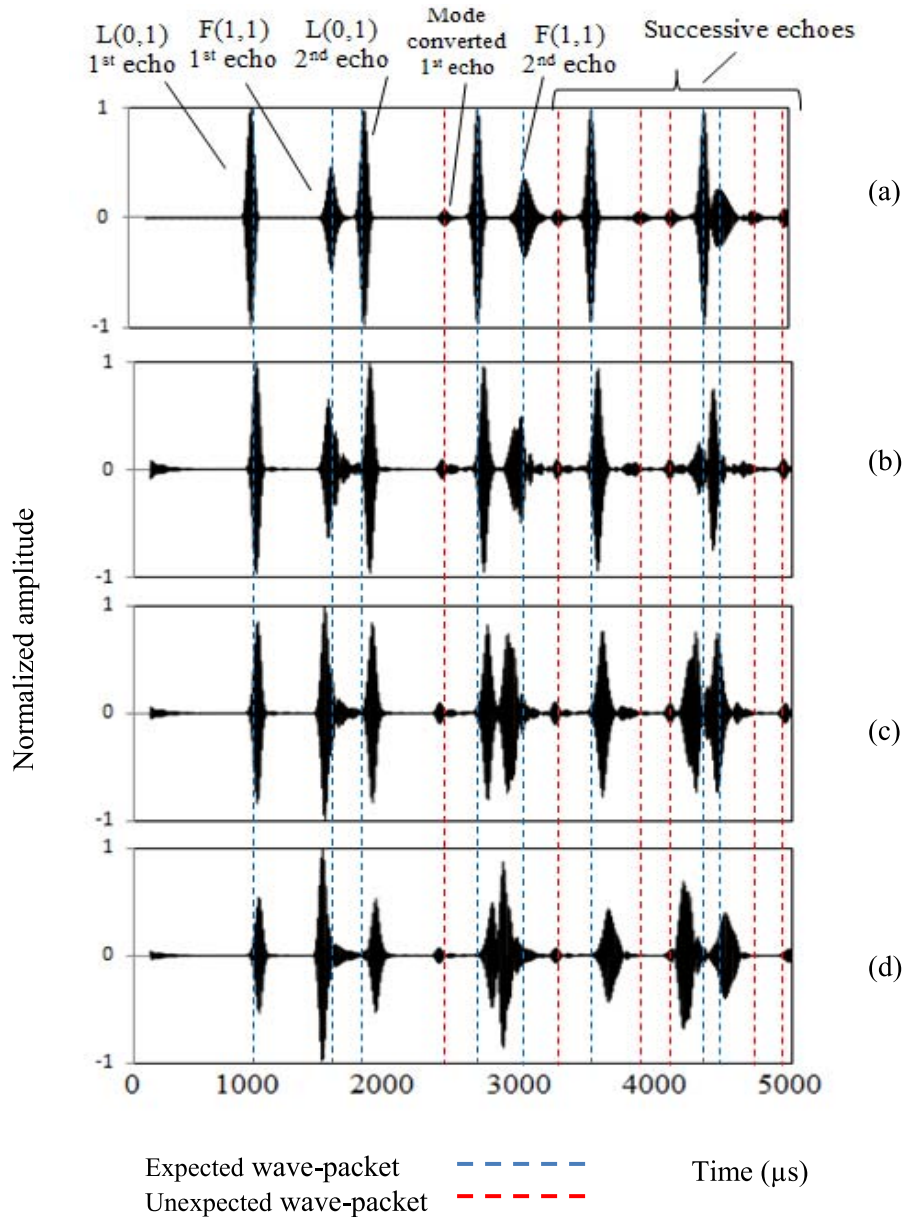
Fig. 4.   Parametric study results, UGW response of: (a) 8 mm, (b) 10 mm, (c) 12 mm, and (d) 14 mm diameter rod.
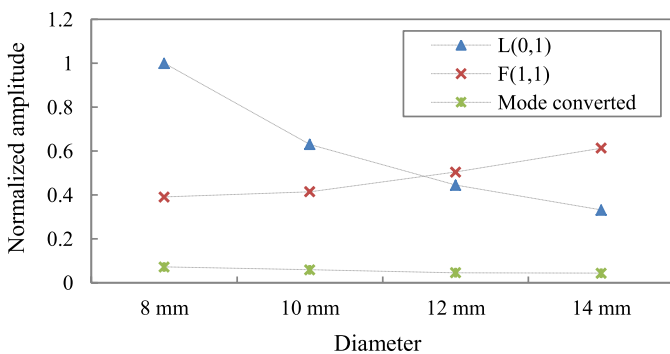

Fig. 5.   Peak amplitude proportions for individual wave modes.

The peak amplitudes of the reflected and mode converted signals off the transducers shown in Figure 4 are extracted, normalized and given in Figure 5. The amplitude change of different guided wave modes depend on the wave mode of interest and also the frequency-thickness product [28]. As can be observed, in FE models, the amplitude of L(0,1) decreases as the rod diameter expands. Therefore, as the diameter of the rod increases the effect is less in generating axisymmetric wave modes by a single transducer. In FE models, the amplitude of F(1,1) increases as the rod diameter expands. When the size of the UGW transmitter is an order of magnitude smaller than the wavelength of the transmitted signal, it could be considered as a point source. According to the alignment of the excitation, it would be expected that all possible modes over the frequency bandwidth of the excitation signal would be generated *i.e.*, L(0,1) and F(1,1). However; as the rod diameter expands, the ratio between the rod diameter and local excitation displacement increases. Therefore, the amplitude of non-axisymmetric wave modes *i.e.*, F(1,1) will have higher contributions to the UGW response [2].

TABLE II
ToA OF INDIVIDUAL MODES AT 80 kHz FOR 8 mm
DIAMETER ALUMINIUM ROD

Mode Type	v_{gr}	FE model ToA	Experiment ToA
L(0,1)	5100 m/s	815 μs	825μs
F(1,1)	2900 m/s	1400 μs	1388 μs
Mode converted	N/A	2205 μs	2290 μs

Fig. 6.   Experimental setup for FEA validation.

In this particular setup (Figure 2), mode conversions occur from a number of different modes propagating in the rod and interacting with the transducer. For this reason it is necessary to have a convenient shorthand system for designating a particular reflected and converted wave modes [7]. The notation adopted for this paper is the following:

- L(0,q) — converted longitudinal mode from F(1,1), q≥ 1
- F(β,q) — converted flexural mode from L(0,1), $\beta \geq 1$
- Mode converted — superposition of mode converted L(0,q) and F(β,q)

The mode converted wave-packet is the superposition of F(β,q) and L(0,q) at the same ToA since their round trip time would be identical while they are interchangeably converted. This has been calculated in which F(β,q) and L(0,q) possess the exact equivalent ToAs as,

$$ToA_{L(0,q)} = ToF_{F(\beta,q)} = 2\left(t_{L(0,1)} + t_{F(1,1)}\right) \qquad (1)$$

where, $t_{L(0,1)}$ and $t_{F(1,1)}$ are the time duration for L(0,1) and F(1,1) respectively to propagate from one free-edge of the rod to the other. The time durations are calculated based on,

$$t = x/v_{gr} \qquad (2)$$

where, x is the propagation distance of the wave mode of interest and v_{gr} is the group velocity value given by the dispersion curve (Figure 3). Therefore, these two mode converted wave-packets are combined to build another wave-packet with relatively higher amplitude with respect to each one of them individually. The individual mode converted wave-packets are extracted by 3D-LDV in Section IV-C.

In order to facilitate the direct extraction of ToA from the individual wave modes, the excitation frequency of 80 kHz was selected. The ToA of individual L(0,1) and F(1,1) at the chosen frequency are summarized in Table-II and agreed in FE models.

IV. LABORATORY EXPERIMENT

Laboratory experiments were performed to validate the presence of mode conversion predicted by the FEA in Section III and also to investigate the mode conversion based on the coupling force. An 8mm diameter, 2.15m long aluminium rod
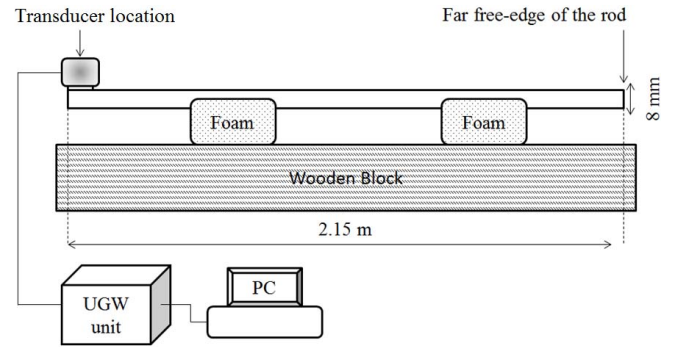
as modelled in the FEA procedure has used to perform these controlled experiments. Existences of the predicted modes are validated using 3D-LDV measurements.

A. Empirical Validation of FEA

The experimental setup is illustrated in Figure 6. An 8 mm diameter, aluminium rod with the length of 2.15 m has been used for the experimental validation. According to the parametric study; the signals could be clearly identified in the selected waveguide since there is no interaction predicted between the individual reflections.

The rod was placed on two wooden blocks and supported with foam to avoid any possible reflection from the surroundings. The transducer is bonded axially to the rod in a manner that allows it to actuate longitudinally. To validate the FE models, an 80 kHz 10 cycle Han-windowed pulse was excited using a UGW unit [22]. The UGW response is displayed in Figure 7-(a). The mode converted signals off the transducer can be observed at multiple echoes and correlates with the result obtained for the 8 mm diameter aluminium rod in the parametric study, Figure 4-(a) which uses a 3D geometry of the transducer for excitation. As was discussed in Section III, this is due to the UGW interaction with the transducer which induces the mode conversion. The experimental result is summarized and compared with *FE model* in Table-II. It is also denoted that there was no mode conversion observed from the far flat free-edge of the rod where no feature was coupled to its surface.

Figure 7-(b) illustrates the UGW response from the same aforementioned experimental setup considering that a *phantom transducer* was coupled to the opposite end of the rod. It is observed that additional unexpected wave-packets exist (as labeled in Figure 7-(b)) as well as the mode converted signals which were also observed in Figure 7-(a). The unexpected wave-packets labeled in Figure 7-(b) are the result of mode conversions from the *phantom transducer* coupled to the opposite end of the rod. Therefore each time the wave modes of interest, L(0,1) and F(1,1) interact with the *phantom transducer* they mode convert interchangeably as denoted in Section-III as L(0,q) and F(β,q). The mode converted wave-packets (L(0,q) and F(β,q)) observed in Figure 7-(b) superpose at the transduction location and appear as a wave-packet possessing a higher amplitude compared to L(0,q) and F(β,q) individually.
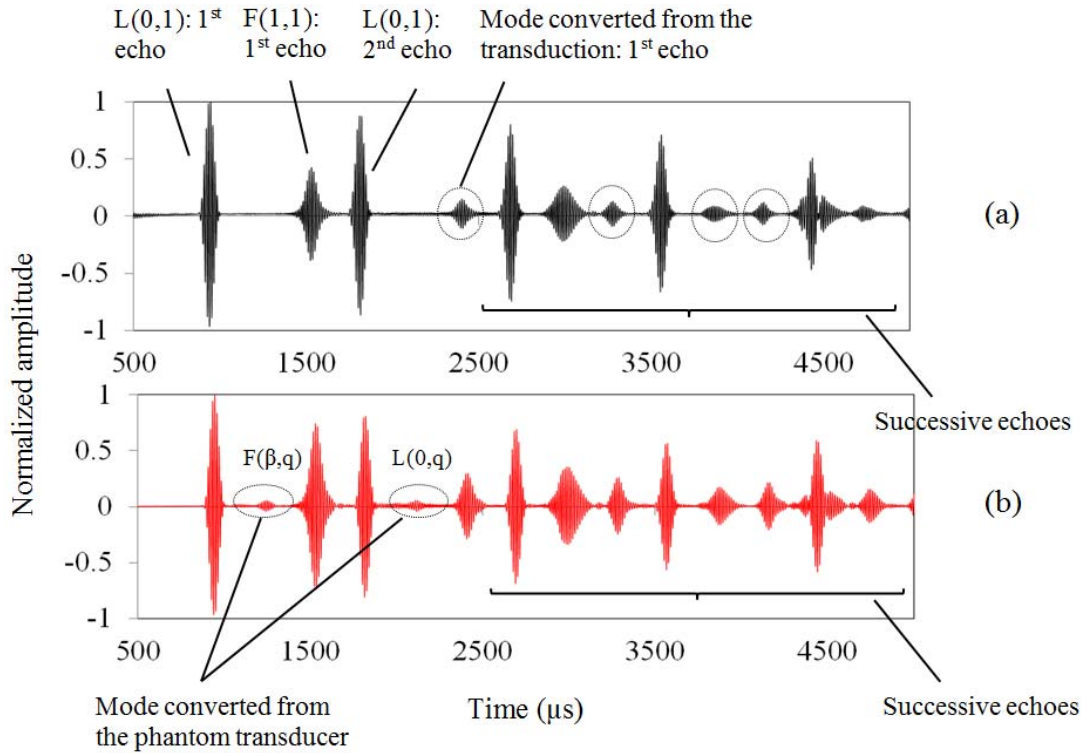
Fig. 7.   UGW response at 80 kHz: (a) pulse echo and (b) pulse echo with a phantom transducer at the opposite end of the rod.

B. Force-Based Coupling Dependent Mode Conversion

As was discussed in Section-II-C, the UGW transducers are commonly dry-coupled using clamps [29], [30], springs [1], [31], pneumatic collars/air pressure [21] to supply a normal loading force. The applied force can affect the amplitude of the UGW response [23]. Therefore, an investigation was conducted to study the effect of a varying physical force applied on a single shear transducer and the subsequent UGW response while transmitting through an aluminium rod and reflecting from its free-edge. In Section IV-B, pulse-echo excitations have been made with an incremental increase in force in order to observe the relationship between the force and the peak amplitude of the first reflected signals from the free-edge of the rod and mode converted signal, from the transducer.

1) Experimental Setup: The test rig which is displayed in Figure 8 is designed to mount transducers and accommodate long lengths of waveguides. The criterion of the rig is to apply a normal force onto the transducer. The force applied can be controlled and varied. The premise of the rig is based on a simply supported beam subjected to a point force. A pneumatically driven ram is used to apply a force. The ram is bolted onto an aluminum truss. It contains an extended shaft that houses the transducer and accurately positions the transducer repeatedly. The force applied is varied by an air pressure regulator with a gauge indicating the pressure supplied to the ram. A toggle switch has been implemented to actuate and retract the ram in order to safely mount and dismount the transducer. Neglecting the self-weight of the beam, any force applied on the waveguide will create an equal but opposite reaction force at the location of contact.
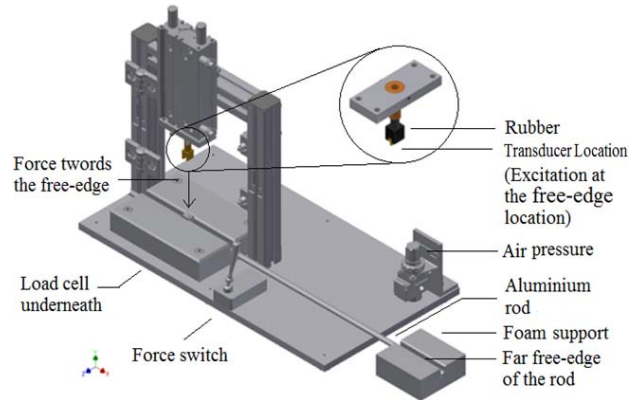

Fig. 8.   Test rig set-up.

This principle was used to measure the force being exerted on the transducer by the pneumatic ram. A load cell sensitive to compression forces is placed directly underneath the waveguide at the location where the transducer is impacting with the waveguide. With the waveguide sitting on the load cell, a reaction force reading can be taken when an external force is applied to the waveguide.

2) Pulse-Echo Excitation With Incremenrtal Applied Forces: Incremental forces were exerted on to the transducer whilst transmitting a pulse at 80 kHz. At this frequency, an UGW response with sufficient wave mode separation is produced according to given velocities and corresponding ToAs given in Table-II. The transmitter is coupled to the free-edge of the rod and the force applied on the transducer is then subsequently adjusted from 5 to 205N with 10N increments. Data collection is taken for the specified frequency
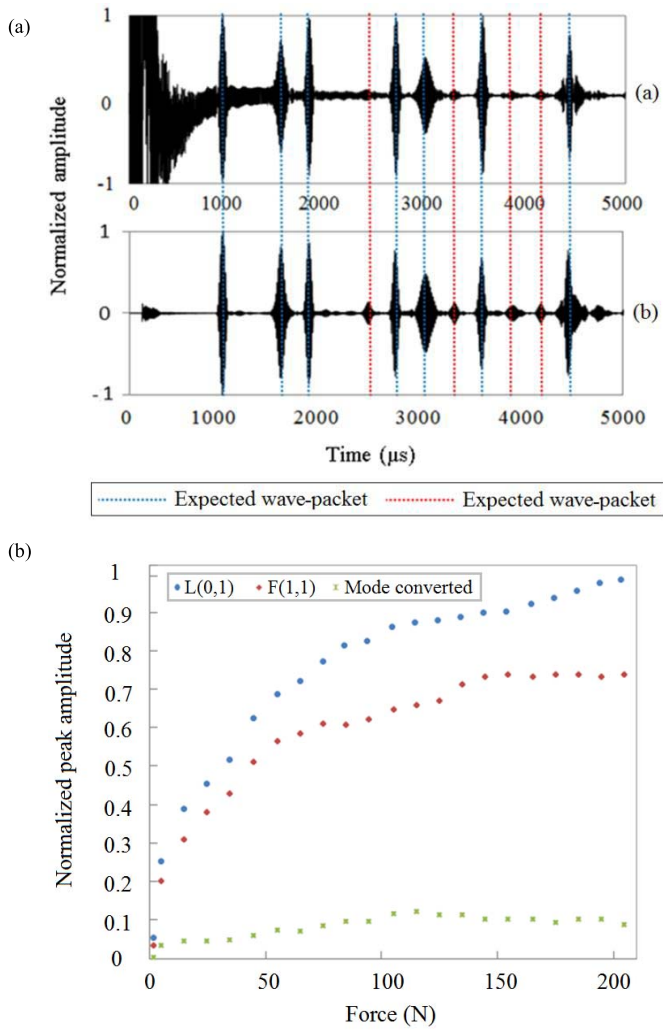
(a)

(b)

Fig. 9. (a) Sample UGW response at (Top) 5 N and (bottom) 55 N applied force. (b) Force versus amplitude of a pulse-echo excitation at 80 kHz for L(0,1), F(1,1) and the mode converted signal from the transduction location.

range for each load cell reading. Two sample pulse-echo UGW responses at 5 and 55N applied forces are displayed in Figure 9-(a) which represents multiple echoes from the far free-edge of the rod. As can be observed in Figure 9-(a)-(Bottom), a wave-packet arises at $2290\,\mu s$ after the first echo of F(1,1) wave mode which is the result of mode conversion from the coupled transducer.

The overall results of the peak amplitude for the first reflected L(0,1), F(1,1) and mode converted signals, are plotted against the incremental rise in clamping force in Figure 9-(b). The test was repeated five times and the standard error of the responses were calculated to be less than 10%. It is illustrated that the amplitude of the mode converted signal non-linearly increases with incremental forces. This behavior can be prescribed from various macroscopic elastic contact theories which are fundamentally based upon the *Hertzian theory of elastic contact*. It is said that the contact area between two elastic bodies is proportionally equivalent to the normal force applied to it by a power of a 1/3 [24], [25].

It is notable that the mode converted signal buries in the coherent noise [32] (SNR $\approx$ 16 dB) at a low force (*i.e.*, 5N). In this case due to the low level of force applied to

the transducer, the coupling will be affected and the UGW response experiences a relatively long ringing phenomenon as can be seen in Figure 9-(a) (Top). The amplitude of the mode converted signal is considerable (*i.e.*, $\approx$19 dB below the first reflected L(0,1) and 17 dB below the first reflected F(1,1) at higher level of forces (*i.e.*, 15 to 205 N). Therefore, above the threshold of a clamping force (*i.e.*, 15 N) the coupled transducer effectively acts as a non-axisymmetric feature in body on the waveguide which has also been observed in Section-III, in the context of Finite Element Analysis and Empirical Validation of *FEA*.

C. 3D - LDV Verification

According to the test-setup used in previous sections, the mode converted signals *i.e.*, L(0,q) & F(β,q) were superposed at the transducer location (*e.g.* Figure 4) in which the consequent wave-packet was labeled as mode converted. Laser vibrometry [25] was used to unintrusively measure the vibration of the surface and separate L(0,q) and F(β,q) wave modes which were superposed at the transducer location of the waveguide. The optical receiver can potentially eliminate the uncertainty of the coupling and receiving transfer function of the piezoelectric ceramic so the existence of wave modes generated purely by transmission could be validated. The 3D-LDV is equipped with three laser sensor heads in order to detect the 3D motions caused by UGW propagation through the structure. The motions of the surface are caused by excitation of 5 cycle UGW signals at 80 kHz by a shear transducer. Thus, the laser can detect the displacement and the surface velocity of wave propagation through the structure with a continuous analog voltage output that is proportional to the target velocity component along the direction of the laser beam [33].

In order to capture the full wave form of the wave modes from the vibrometry results, 0.36m of the rod was scanned based on Equation-3. Although a 10 cycle Hann windowed sine wave was used in the FE model and experimental validation (Section-III and IV), the excitation of 5 cycles was alternatively performed in the vibrometry experiment due to the limitation of the beam angle of the laser heads [33]. Given the velocity and excitation frequency of the existing wave modes, the longest possible pulse-length (L) could be calculated as,

$$L = n\lambda \qquad (3)$$

where, n is the number of cycles and λ is the wavelength of the wave mode of interest which can be expressed as,

$$\lambda = v_{gr\_max}/f \qquad (4)$$

where, v_{gr_max} is the maximum group velocity value of the existing wave modes across the operating frequency range. Therefore, the sufficient length of line scan could be chosen as a value equivalent or more than L.

1) Scan Setup: The same aforementioned pulse-echo excitation setup illustrated in Section-III has been used during the vibrometry scan, taking into account that a *dividing head* was used to rotate the waveguide eight times with
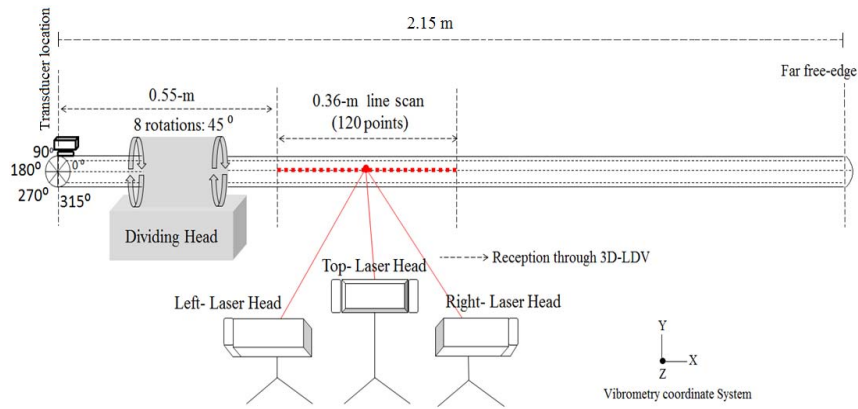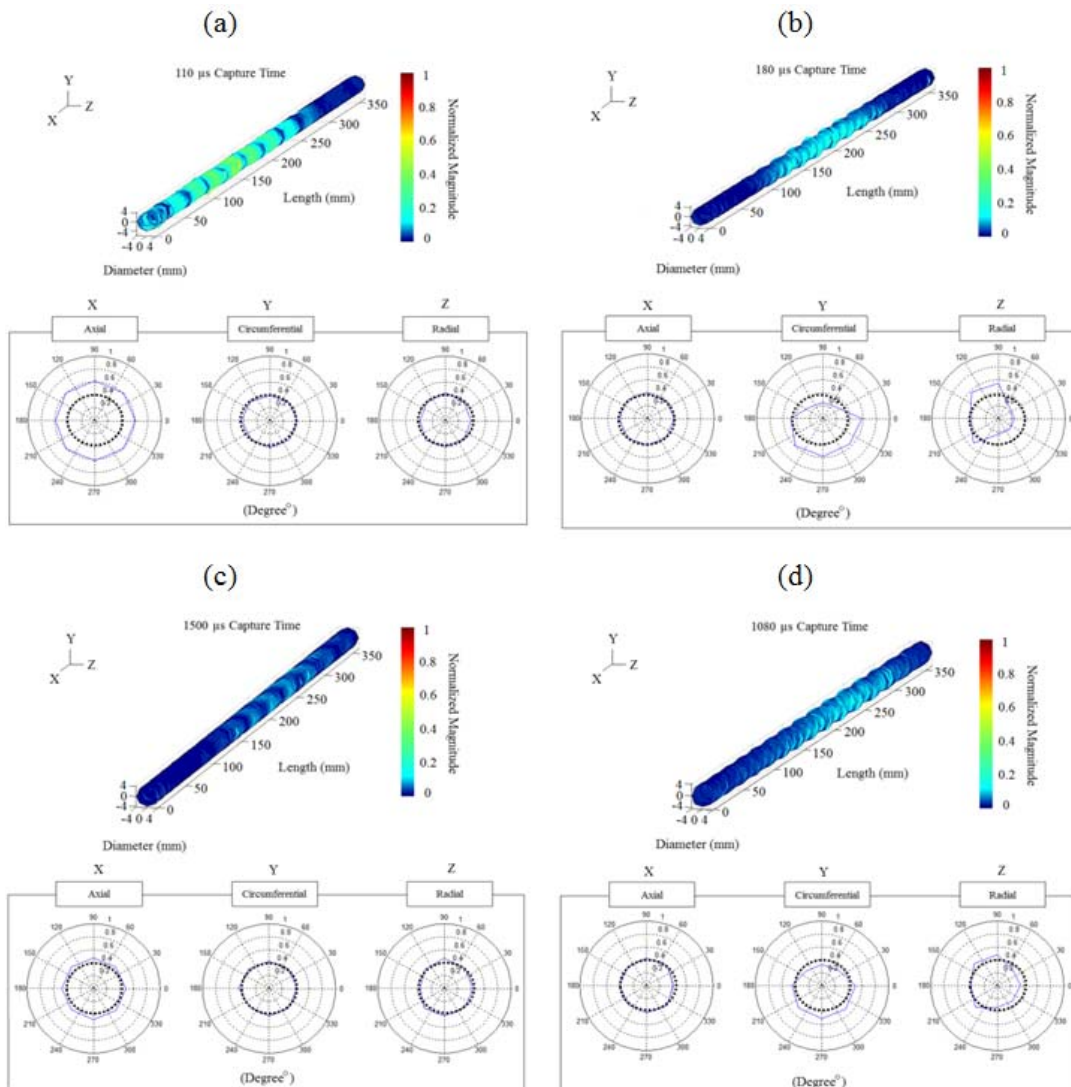
Fig. 10.   3D-LDV setup.

Fig. 11.   Identified wave modes: (a) L(0,1), (b) F(1,1), (c) L(0,q), and (d) F(β,q) using 3D-LDV.

45° intervals. Therefore, eight 3D-line scans with 120 points have been conducted covering 0.36m of the rod at each individual degree as illustrated in Figure 10. According to the dispersion curve given in Figure 3, the L(0,q) and F(β,q) could be potentially separated along the line scan, 0.55m away from the excitation point since the 3D-LDV can act as a non-contact UGW receiver. Foam was used beneath the rod and inside the *dividing head* in order to prevent the *dividing head* from causing any additional feature to the waveguide's surface.

2) Scan Results and Analysis: Figure 11 represents the surface velocity of the waveguide at a fixed point in time (in isometric and cross-sectional view) caused by various UGW modes. The polar plots represent the cross sectional view of the measured axial, circumferential and radial displacement respectively for each mode. Figure 11 provides normalized measurements of surface velocity of the waveguide at the points where the lasers are pointed. A measurement of this kind provides a signal that represents the material's velocity at the surface of the waveguide as recorded over time. Since the velocity is the rate of displacement, it is possible to use either when measuring the characteristics of the wave modes. Note that the surface velocity does not represent the propagating velocity of the wave modes. Four wave modes *i.e.*, L(0,1), F(1,1), L(0,q) and F(β,q) are displayed in Figure 11 and identified according to their displacement characteristics (Section II-A), measure of dispersion (Figure 3), expected ToAs (Equation-2) and estimated pulse length (Equation-3). The wave modes present in the waveguide which were identified by the 3D-LDV correlated with the reflected and converted modes identified throughout the modeling and experimentation. It was also validated that the modes known as L(0,q) and F(β,q) will be added to the UGW response due to mode conversion as was also predicted in Section-III and IV.

A mode converted signal generated by a transmitter emulating a waveguide feature is influenced by two main governing factors. Primarily, the amplitude of an original mode directly affects the presence of a mode converted signal from a feature as it is a derivative from the initial incident wave. The second factor is that the occurrence of mode conversion is dependent on the ability of a transducer to act as a non-axisymmetric feature on a structure.

This phenomenon can make the signal interpretation challenging as in some applications it has the potential to be misread with the structural elements of the waveguide due to reverberation of the incident wave mode with different known features. Therefore, based on the SNR resolution of the guided wave systems these interacting wave modes with the transducers may appear in the guided wave response overlapping with other wave modes reflected from different structural elements. In addition, the phenomenon can be misinterpreted and/or superposed with some higher order modes existing in the operating frequency region especially in some applications where the cut-off frequency of the higher order longitudinal/flexural modes are relatively low, *e.g.* 68 kHz for an 64 mm diameter aluminium rod.

V. CONCLUSION

In this paper UGWs interacting with the piezoelectric transducers were reported and studied. The wave mode proportions were quantified when applying different incremental coupling forces to the transducer. The study demonstrated that the dry-coupled transducer on the waveguide can act as a non-axisymmetric feature which subsequently contributes to the presence of extra wave-packets appearing in the guided wave response. Further results indicated that the amplitude of the mode converted signal increases non-linearly with respect to the incremental force. This amplitude at a low force (*i.e.*, 5 N) was negligible in which it was masked by the noise. In this case due to the level of force applied to the transducer, the coupling between the transducer and the waveguide was nominal and the guided wave response experienced a relatively long ringing phenomenon. In addition, according to the parametric study, the magnitude of the reflections and mode conversions off the transducers reduces when the waveguide diameter expands. The same effect has been appreciated on the fundamental longitudinal propagating wave modes *i.e.*, $L(0, 1)$ and the reverse effect has been understood on the fundamental flexural wave mode *i.e.*, $F(1, 1)$ in the aluminium rod under investigation.

The 3D-LDV was used to identify and separate the wave modes of interest which confirmed that the longitudinal wave mode converted to flexural wave mode and contrariwise at each echo when interacting with the transducer.

In conclusion, since the reflected and mode converted signals off the transducers are quantified in this study; the outcome could be used to predict the same effect on other scenarios such as research laboratory experiments and field inspections. This phenomenon can make the interpretation of the guided wave response challenging as in some applications it has the potential to be misread with the structural elements of the waveguide due to reverberation of the incident wave mode with different known features. Therefore, based on the SNR resolution of the guided wave systems these interacting wave modes with the transducers may appear in the guided wave response overlapping with other wave modes reflected from different structural elements and contribute to the coherent noise.

Future studies may include the quantification of the reported phenomenon on other types of structures with different array designs.

REFERENCES

[1] J. L. Rose, "An introduction to ultrasonic guided waves," in *Proc. 4th Middle East NDT Conf. Exhibit.*, Kingdom of Bahrain, Bahrain, Dec. 2007, pp. 1–18.

[2] P. P. Catton, "Long range ultrasonic guided waves for the quantitative inspection of pipelines," Ph.D. dissertation, Dept. Eng., Brunel Univ., Uxbridge, U.K., 2009, pp. 1–141.

[3] D. W. Greve, H. Sohn, C. P. Yue, and I. J. Oppenheim, "An inductively coupled Lamb wave transducer," *IEEE Sensors J.*, vol. 7, no. 2, pp. 295–301, Feb. 2007.

[4] J. L. Rose, "Successes and challenges in ultrasonic guided waves for NDT and SHM," in *Proc. Nat. Seminar Exhibit. Non-Destruct. Eval.*, Tiruchirappalli, India, Dec. 2009, pp. 1–9.

[5] S. Fateri, N. V. Boulgouris, A. Wilkinson, W. Balachandran, and T.-H. Gan, "Frequency-sweep examination for wave mode identification in multimodal ultrasonic guided wave signal," *IEEE Trans. Ultrason., Ferroelectr., Freq. Control*, vol. 61, no. 9, pp. 1515–1524, Sep. 2014.

[6] G. P. Devault and C. W. Curtis, *J. Acoust. Soc. Amer.*, vol. 635, no. 31, 1959.

[7] A. H. Meitzler, "Mode coupling occurring in the propagation of elastic pulses in wires," *J. Acoust. Soc. Amer.*, vol. 33, no. 4, pp. 435–445, 1961.

[8] D. N. Alleyne, M. J. S. Lowe, and P. Cawley, "The reflection of guided waves from circumferential notches in pipes," *J. Appl. Mech.*, vol. 65, no. 3, pp. 635–641, 1998.

[9] M. J. S. Lowe, R. E. Challis, and C. W. Chan, "The transmission of Lamb waves across adhesively bonded lap joints," *J. Acoust. Soc. Amer.*, vol. 107, no. 3, pp. 1333–1345, 2000.

[10] A. Demma, P. Cawley, M. Lowe, and A. G. Roosenbrand, "The reflection of the fundamental torsional mode from cracks and notches in pipes," *J. Acoust. Soc. Amer.*, vol. 114, no. 2, pp. 611–625, Aug. 2003.

[11] Y. Cho, "Estimation of ultrasonic guided wave mode conversion in a plate with thickness variation," *IEEE Trans. Ultrason., Ferroelectr., Freq. Control*, vol. 47, no. 3, pp. 591–603, May 2000.

[12] Y. Cho and J. L. Rose, "A boundary element solution for a mode conversion study on the edge reflection of Lamb waves," *J. Acoust. Soc. Amer.*, vol. 99, no. 4, pp. 2097–2109, 1996.

[13] B. Morvan, N. Wikie-Chancellier, H. Duflo, A. Tinel, and J. Duclos, "Lamb wave reflection at the free edge of a plate," *J. Acoust. Soc. Amer.*, vol. 113, no. 3, pp. 1417–1425, 2002.

[14] Y. Jiangong, W. Bin, and H. Cunfu, "Guided circumferential waves in orthotropic cylindrical curved plate and the mode conversion by the end-reflection," *Appl. Acoust.*, vol. 68, no. 5, pp. 594–602, 2007.

[15] P. S. Lowe, S. Fateri, R. Sanderson, and N. V. Boulgouris, "Finite element modelling of the interaction of ultrasonic guided waves with coupled piezoelectric transducers," *Insight-Non-Destruct. Test. Condition Monitor.*, vol. 56, no. 9, pp. 505–509, 2014.

[16] W. B. Na and H. S. Yoon, "Wave-attenuation estimation in fluid-filled steel pipes: The first longitudinal guided wave mode," *Russian J. Nondestruct. Test.*, vol. 43, no. 8, pp. 549–554, 2007.

[17] M. G. Silk and K. F. Bainton, "The propagation in metal tubing of ultrasonic wave modes equivalent to Lamb waves," *Ultrasonics*, vol. 17, no. 1, pp. 11–19, 1979.

[18] R. M. Sanderson and S. D. Smith, "The application of finite element modelling to guided wave testing systems," in *Proc. AIP Conf., Rev. Quant. Nondestruct. Eval.*, vol. 22. 2003, pp. 256–263.

[19] K. Sezawa, "Anomalous dispersion of elastic surface waves II," *Bull. Earthquake Res. Inst.*, vol. 16, pp. 225–233, Nov. 1938.

[20] H. Cui, J. Trevelyan, and S. Johnstone, "Anomalous dispersion of flexural guided waves in clad rods," *IEEE Trans. Ultrason., Ferroelectr., Freq. Control*, vol. 58, no. 7, pp. 1525–1528, Jul. 2011.

[21] G. R. Edwards and T.-H. Gan, "Detection of corrosion in offshore risers using guided ultrasonic waves," in *Proc. ASME 26th Int. Conf. Offshore Mech. Arctic Eng. (OMAE)*, San Diego, CA, USA, Jun. 2007, pp. 377–384.

[22] Plant Integrity Ltd., "Teletest focus long range ultrasonic system specification," TWI—The Welding Institute Cambridge, U.K., Tech. Rep., Feb. 2007.

[23] D. N. Alleyne and P. Cawley, "The excitation of Lamb waves in pipes using dry-coupled piezoelectric transducers," *J. Non-Destruct. Eval.*, vol. 15, no. 1, pp. 11–20, 1996.

[24] J. A. Greenwood, "On the DMT theory," *Tribol. Lett.*, vol. 26, no. 3, pp. 203–211, 2007.

[25] K. L. Johnson, *Contact Mechanics*. Cambridge, U.K.: Cambridge Univ. Press, 1987, pp. 1–468.

[26] B. Pavlakovic, M. Lowe, D. Allyeyne, and P. Cawley, "Disperse: A general purpose program for creating dispersion curves," in *Review of Progress in Quantitative Nondestructive Evaluation*. New York, NY, USA: Springer, 1997.

[27] C. R. Fuller, "The effects of wall discontinuities on the propagation of flexural waves in cylindrical shells," *J. Sound Vibrat.*, vol. 75, no. 2, pp. 207–228, 1981.

[28] J. L. Rose, *Ultrasonic Waves in Solid Media*. Cambridge, U.K.: Cambridge Univ. Press, 2004, p. 114.

[29] P. D. Wilcox, "A rapid signal processing technique to remove the effect of dispersion from guided wave signals," *IEEE Trans. Ultrason., Ferroelectr., Freq. Control*, vol. 50, no. 4, pp. 419–427, Apr. 2003.

[30] M. J. S. Lowe and P. Cawley, "Long range guided wave inspection usage—Current commercial capabilities and research directions," Dept. Mech. Eng., Imperial College, London, U.K., Mar. 2006, pp. 1–40. [Online]. Available: http://www3.imperial.ac.uk/pls/portallive/docs/1/55745699.PDF

[31] J. L. Rose, "Ultrasonic guided waves in structural health monitoring," *Key Eng. Mater.*, vols. 270–273, pp. 14–21, Aug. 2004.

[32] P. Cawley and D. N. Alleyne. (Feb. 2004). *Practical Long Range Guided Wave Inspection—Managing Complexity*. [Online]. Available: http://www.ndt.net/article/mendt03/4/4.htm, accessed Oct. 9, 2014.

[33] D. E. Oliver, "Tutorial: 3D scanning vibrometry for structural dynamics measurements," IMAC XXVII, Polytec, Inc., Hamburg, Germany, Tech. Rep., 2007.

Sina Fateri was born in Babol, Iran. He received the B.Sc. (Hons.) degree in computer science from the University of Mazandaran, Babolsar, Iran, in 2009, and the M.Sc. (Hons.) degree in wireless communications engineering from Brunel University London, U.K., in 2011, where he is currently pursuing the Ph.D. degree in electronic systems research based at TWI Ltd., Cambridge, U.K. He was a Graduate Teaching Assistant with the Wireless Communications Laboratory from 2011 to 2013. Since 2015, he has been a Project Leader with Plant Integrity Ltd., where he is performing signal processing for industrial sectors. His research is focused on advanced signal processing techniques for ultrasonic guided wave inspections. His research interests are acoustic signal processing, mode identifications in ultrasonic guided wave inspections, and ultrasonic guided wave mode conversion from discontinuities.

Premesh Shehan Lowe was born in Colombo, Sri Lanka, in 1987. He received the B.Sc. (Hons.) degree in computer science and software engineering from Edith Cowan University, Perth, Australia, in 2008, and the M.Sc. degree in electrical and network engineering from the University of Hertfordshire, Hatfield, U.K., in 2012. He is currently pursuing the Ph.D. degree in electrical and computer engineering at Brunel University London, U.K. In 2012, he joined the Integrity Management Group, TWI Ltd., U.K., as a Ph.D. Research Engineer. His research is focused on finite-element methods and signal processing of ultrasonic guided wave (UGW) inspection. His research interests are to develop novel UGW transducers to achieve higher flaw sensitivity and UGW energy focusing.

Bhavin Engineer received the B.Eng. (Hons.) degree in aerospace engineering from Queen Marys and Westfield College, University of London, in 2006, and the M.Sc. (Hons.) degree in engineering design from Brunel University London, in 2009. From 2009 to 2013, he was a Research Engineer with TWI/Plant Integrity Ltd while working towards a Ph.D. degree. His Ph.D. degree was involved in empirically characterizing the mechanical behavior of ultrasonic guided wave (UGW) transducers and creating resonant finite element analysis models of UGW transducers. Since 2013, he has been involved in a design and development capacity for plant integrity in producing UGW products for oil and gas pipeline testing.

Nikolaos V. Boulgouris (S'96–M'04–SM'09) received the Ph.D. degree from the Electrical and Computer Engineering Department, University of Thessaloniki, Greece, in 2002. From 2003 to 2004, he was a Post-Doctoral Fellow with the Department of Electrical and Computer Engineering, University of Toronto, Canada. From 2004 to 2010, he served as a Lecturer and Senior Lecturer with King's College London, London, U.K. He is currently a Senior Lecturer with the Department of Electronic and Computer Engineering, Brunel University London, U.K. He served as a Guest Co-Editor of two journal special issues, and was a Co-Editor of a book entitled *Biometrics: Theory, Methods, and Applications* (Wiley-IEEE Press, 2009). He served as an Associate Editor of the IEEE TRANSACTIONS ON IMAGE PROCESSING from 2010 to 2014, and the IEEE SIGNAL PROCESSING LETTERS from 2007 to 2011.